Journal of Physics: Conference Series

PAPER • **OPEN ACCESS**

Design of a Dual-Band Planar Inverted F-L Implantable Antenna for Biomedical Applications

To cite this article: Sanaa Salama *et al* 2020 *J. Phys.: Conf. Ser.* **1711** 012002

Design of a Dual-Band Planar Inverted F-L Implantable Antenna for Biomedical Applications

Sanaa Salama[1], Duaa Zyoud[2], and Ashraf Abuelhaija[3]

[1,2] Telecommunication Engineering Department, Arab American University, Jenin, Palestine.
[3] Electrical Engineering Department, Aplied Scince Private University, Amman, Jordan.

Corresponding author's email address: sanaa.salama@aaup.edu

Abstract. In this paper, a dual-band planar inverted F-L implantable antenna, which operates at theMedical Implant Communications Services (MICS) and Industrial, Scientific, and Medical (ISM) bands, is introduced. The proposed antenna is printed on RO3010 substrate of thickness 2mm, relative permittivity 10.2, and loss tangent 0.0023. A short-circuit pin inserted between the ground plane and the patch is used to downsize the antenna. The dimension of the antenna is 27× 19×2 mm^3. The proposed implantable antenna covers a frequency band of 9.4 MHz [397-406.4 MHz] at MICS band with a return loss of -20.02dB at 403 MHz and a frequency band of 80 MHz [2.41-2.49 GHz] at ISM band with a return loss of -22.82 at 2.45 GHz. Design and analysis of the proposed antenna is carried out by Computer Simulation Technologies (CST) Microwave studio.

1. Introduction

Designing implantable antennas to work in human tissue is a challenge. Parameters such as low power requirements, antenna size, biocompatibility, high tissue conductivity, and impedance matching have to be considered carefully in the design. Several techniques are used to minimize the size of antennas. The most common one is by inserting a short-circuit pin between the radiator and the ground plane. By this technique, the antenna size is halved while keeping the same frequency response, [1,2]. The bandwidth of the antenna can be improved by using a superstrate of high relative permittivity, [3]. In [4], a compact dual-band implantable antenna was presented. The introduced antenna was printed on RO3210 with a size of 22× 16× 1.27mm^3 and working at both MICS and ISM bands. The dual-band antenna was obtained based on modifying and then optimizing a conventional E-shaped planar antenna to cover both the MICS and ISM frequency bands. In [3], a small size dual-band implantable antenna was presented for continuous glucose-monitoring applications. The proposed antenna was fabricated and measured in gels mimicking the electrical properties of human skin. In [5], a dual-band implantable antenna covers both the MICS and ISM bands was presented. The size of the proposed antenna was reduced by using high relative permittivity substrate and superstrate, inserting short-circuit pin, and using spiral shape to increase the length of the current path. In [6], a compact dual-band implantable antenna was introduced for biomedical applications. A short-circuit pin was used for size reduction purposes. For the antenna to be matched at the desired frequency, this was done by creating a U-shaped slot in the ground plane. In [7], a dual-band implantable antenna covers the MICS and ISM bands were introduced. As compared to previous dual-band implantable antennas, the introduced antenna was chosen to be circular shape for eliminating sharp edges that may hurt the surrounding tissues during implantation. To guarantee stable data connection, a dual-band implantable antenna with wider bandwidth was presented in [8]. On the other hand, a tiny size dual-band implantable antenna 9.8mm^3 was presented in [9]. The proposed antenna exhibits a dual-band for both 915 MHz and 2.45 GHz ISM bands. In [10], a compact triple-band implantable antenna was presented. The proposed antenna covers the midfield band (1824–1980 MHz) and the ISM bands (902–928 MHz and 2400–2483.5 MHz). The system architectures are a capsule type to be implanted in deep tissue and a flat type to be implanted in the skin. In this paper, the work in [11] was expanded to obtain a dual-band implantable antenna. In [11] a planar inverted F-implantable antenna was designed using the MICS band. The proposed antenna operates at 403MHz and covers a frequency bandwidth of 1MHz at -10 dB. To operate at ISM band in addition to the MICS band, a planar inverted L-shaped microstrip line is inserted and the whole structure is optimized to obtain a dual-band implantable antenna that covers the MICS and ISM bands.

2. Antenna Design Geometry

The antenna introduced in this paper is designed to be a dual-band implantable antenna by inserting a planar inverted L-shaped microstrip line to the planar inverted F-shaped antenna that was proposed in [11].The structure of the presented antenna is seen in Figure 1. The antenna is built on a 27 × 19 × 2mm^3 RO3010 substrate with a relative permittivity of 10.2, a thickness of 2mm, and a loss tangent of 0.0023. The use of a high dielectric constant substrate causes a decrease in the resonant frequency. To further antenna size reduction, a short-circuit pin is inserted between the patch and the ground plane. The antenna is excited by 50-ohm feed. The length of the planar inverted L-shaped microstrip line is a half-wavelength that resonates at 2.45 GHz. While, due to the short-circuit pin, the length of the planar inverted F-shaped microstrip line is a quarter-wavelength that resonates at 403 MHz. The introduced antenna is implanted in human skin. To model the human skin, tissue dielectric properties in [12] are used. For safety issues and to prevent direct contact between the radiating patch and the human tissue, Alumina superstrate with (relative permittivity = 9.4, tanδ = 0.006, and thickness 0.15mm) is used.

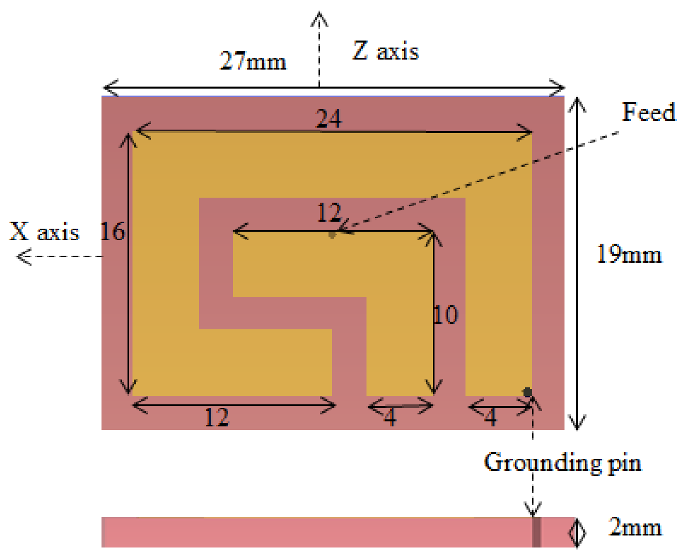

Figure 1. Structure of the dual-band planar inverted F-L implantable antenna. Top and side view.

3. Results and Analysis

The antenna is built and simulated using CST Microwave studio. Figure 2 shows the return loss of the antenna. As can be seen,the presented antenna covers a dual-band with a frequency bandwidth of 9.4 MHz [397-406.4 MHz] at MICS band with a return loss of -20.02 dB at 403 MHz and 80 MHz [2.41-2.49 GHz] at the ISM band with a return loss of -22.82 dB at 2.45 GHz. To ensure safety issue, the average Specific Absorption Rate (SAR) is restricted to 1.6 W/kg for C95.1-1999 and for C95.1-2005 standard, it is restricted to 2 W/kg. The simulated SAR value,the input power is 1 W, at 403 MHz is 27.88W/kg for (1g) standard. Similarly, the simulated SAR value at 2.45 GHz is 28. 08 W/kg (1 g). To ensure safety rules, the maximum input power has to be not more than57.3mW (1 g) at 403 MHz for the MICS band and not more than 56.9mW (1 g) at 2.45 GHz for the ISM band. The simulated SAR values for (1g) standard at 403 MHz and 2.45 GHz are presented in Figure 3. Figure 4 shows the simulated surface current densities at 403 MHz for the MICS band and at 2.45 GHz for the ISM band. At 403 MHz, the peak value of the current density, as can be seen, is found to be concentrated mostly on the planar inverted F-shaped microstrip line, while at 2.45 GHz, the peak current values are mostly concentrated at the planar inverted L-shaped microstrip line. The electric field intensity has its maximum strength on the planar inverted F-shaped microstrip line at 403 MHz. While the field peak value at 2.45 GHz occurs on the planar inverted L-shaped microstrip line, as can be seen from Figure 5.

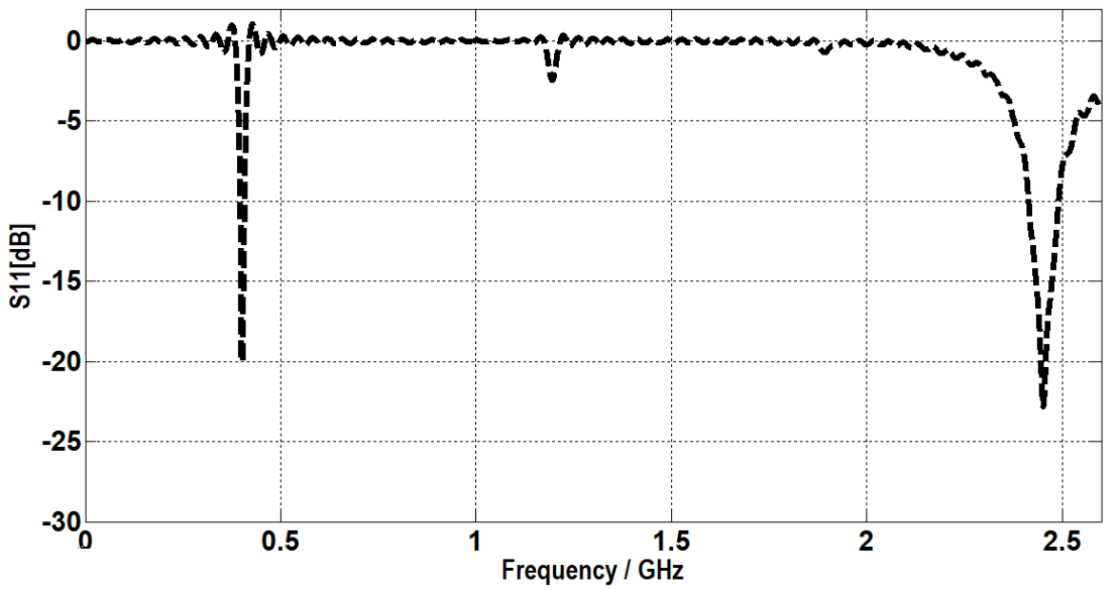

Figure 2. Return loss of the dual-band planar inverted F-L implantable antenna.

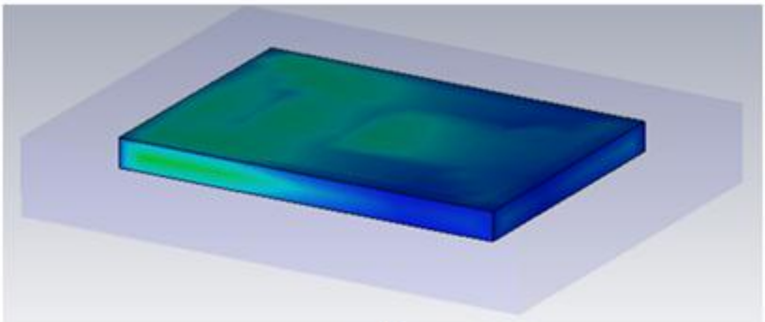

(a)

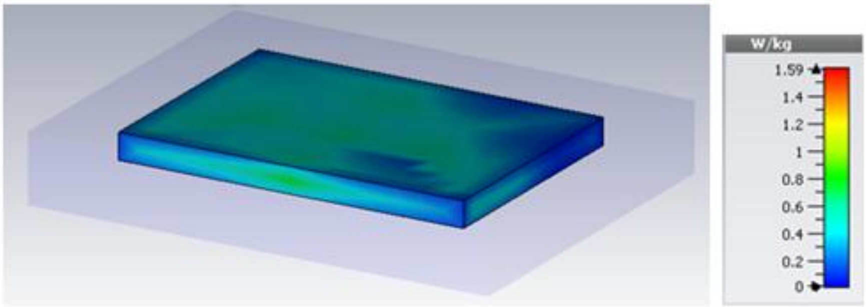

(b)

Figure 3. Simulated SAR value of the dual-band planar inverted F-L implantable antenna at: (a) 403 MHz and (b) 2.45 GHz.

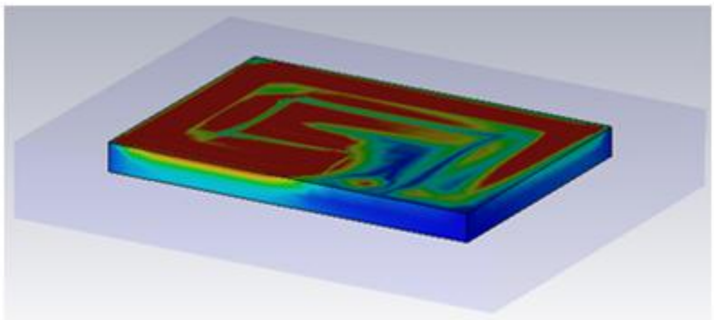

(a)

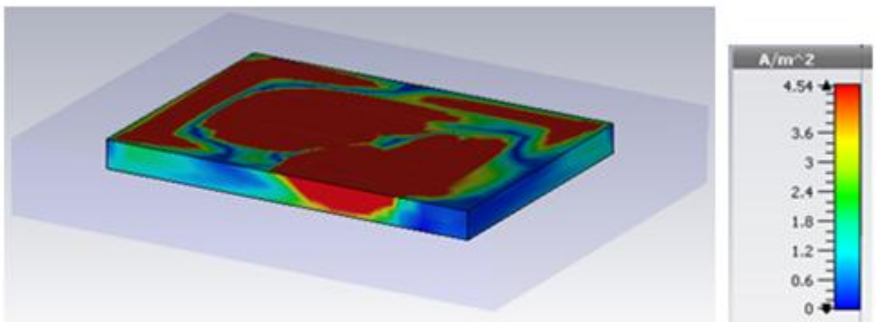

(b)

Figure 4. Current Density of the dual-band planar inverted F-L implantable antenna at: (a) 403 MHz and (b) 2.45 GHz.

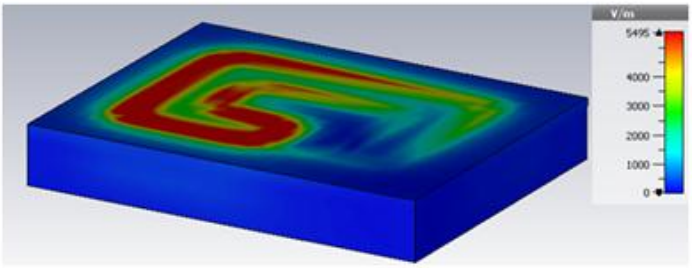

(a)

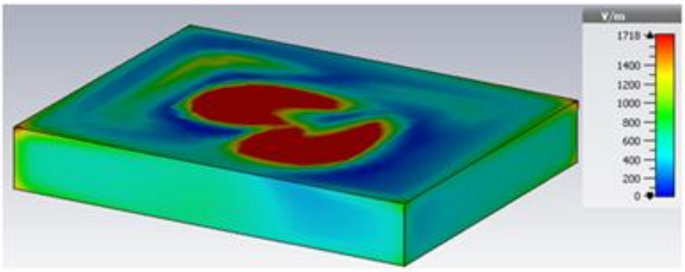

(b)

Figure 5. Electric field intensity of the dual-band planar inverted F-L implantable antenna at: (a) 403 MHz and (b) 2.45 GHz.

Figure 6 displays the simulated far-field patterns for both azimuth plane (theta = 90) and elevation plane (phi = 0) at 403 MHz and 2.45 GHz. For both bands, the antenna patterns are mostly directed away from the body. The antenna exhibits omnidirectional patterns at 403 MHz for both azimuth and elevation planes. While at 2.45 GHz, the radiation patterns are bidirectional for both azimuth and elevation planes. The calculated gain for MICS band at 403 MHz is -30.14 dBi, and the ISM band at 2.45 GHz is 2.45 dBi.

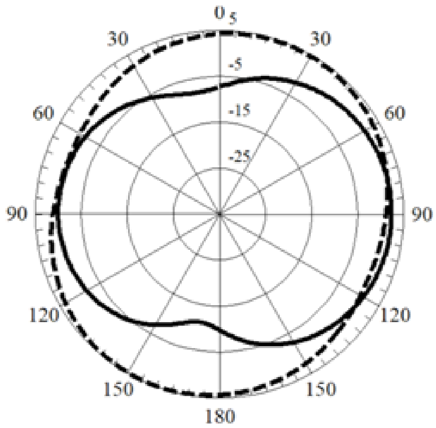

(a)

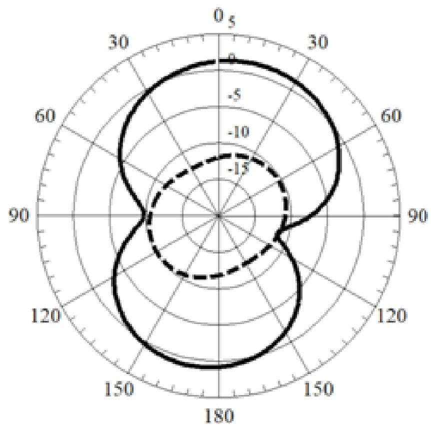

(b)

Figure 6. Far-field patterns of the dual-band planar inverted F-L implantable antenna at: (a) Azimuth plane at 403 MHz (dash line) and 2.45 GHz (solid line), and (b) Elevation plane at 403 MHz (dash line) and 2.45 GHz (solid line).

4. Conclusion

In this paper, a dual-band planar inverted F-L implantable antenna is designed and simulated using CST to work for both the MICS and ISM bands. The antenna size is 27×19×2 mm^3, printed on RO3010 substrate. To prevent direct contact with human tissue, an Alumina superstrate of thickness 0.15 mm is used. A return loss of -20.02 dB at 403 MHz for MICS band and -22.82 dB at 2.45 GHz for ISM band is obtained. For safety issues, this required that the maximum input power has to be not more than 57.3 mW (1 g) at 403 MHz for the MICS band and 56.9mW (1 g) at 2.45 GHz for the ISM band. The far-field patterns for both bands are also simulated. At both frequency bands, the far-field patterns aremostly directed away from the body. At MICS band, the radiation patterns at both azimuth and elevation planes are omnidirectional. While at ISM band, the patterns are bidirectional at both azimuth and elevation planes.

References

[1] Qi Z, Kan F, Tie-zhu L. Analysis of planar inverted-f antenna using equivalent models. *In IEEE AP-S Int. Symp./USNC/URSI Meeting*, 2005, vol. 3A, pp. 142–145.

[2] Huynh C, Stutzman W. Ground plane effects on planar inverted-f antenna (PIFA) performance. *Proc. Inst. Elect. Eng.—Microw., Antennas, Propag.*, 2003, vol. 150, no. 4, pp. 209–213.

[3] Karacolak T, Hood A, Topsakal E. Design of a Dual-Band Implantable Antenna and Development of Skin Mimicking Gels for Continuous Glucose Monitoring. *IEEE Transactions on Microwave Theory and Techniques*, 2008, vol. 56, no. 4, 1001-1008.

[4] Yeap K, Voon C, Hiraguri T, and Nisar H. A Compact Dual-Band Implantable Antenna for Medical Telemetry. *Microw Opt Technol Lett*., 2019, 61, pp.2105–2109. https://doi.org/10.1002/mop.31871.

[5] Basir A, Bouazizi A, Zada M, Iqbal A, Ullah S, Naeem U. A Dual-Band Implantable Antenna with Wide-Band Characteristics at MICS and ISM Bands. *Microw Opt Technol Lett*. 2018, PP.1–5. https://doi.org/10.1002/mop.31447.

[6] Usluer M, Basaran S. Dual Band Implantable Antenna for Biomedical Applications. 2016 URSI *International Symposium on Electromagnetic Theory (EMTS)*.

[7] Kiourti A, Psathas K, Costa J, Fernandes C , Nikita K. Dual-Band Implantable Antennas for Medical Telemetry: A Fast Design Methodology and Validation for Intra-Cranial Pressure Monitoring. *Progress In Electromagnetics Research*, 2013, vol. 141, pp. 161–183.

[8] Hashemi S, Rashed-Mohassel J. Design and miniaturization of dual band implantable antennas. *Biocybern Biomed Eng*, 2018, https://doi.org/10.1016/j.bbe.2018.06.008.

[9] Faisal F, Zada M, Ejaz A, Amin Y, Ullah S, Yoo H. A Miniaturized Dual-band Implantable Antenna System for Medical Applications. IEEE *TRANSACTIONS ON ANTENNAS AND PROPAGATION*, 2019, DOI 10.1109/TAP.2019.2938591.

[10] Zada M, Yoo H. A Miniaturized Triple-Band Implantable Antenna System for Bio-Telemetry Applications. *IEEE TRANSACTIONS ON ANTENNAS AND PROPAGATION*, 2018, vol. 66, no. 12, pp. 7378-7382.

[11] Salama S, Zyoud D, Daghlas R, Abuelhaija A.Design of a Planar Inverted F-Antenna for Medical Implant Communications Services Band.*International Conference on Mathematics, Engineering, Science and Technology 2020, 19-20 SEPT 2020*. (accepted)

[12] Fan Y, Liu X, Li J, Chang T. A Miniaturized Circularly-Polarized Antenna for In-Body Wireless Communications.*Micromachines 2019*, 10, 70; doi:10.3390/mi10010070.